Research Article | Vol. 33, No. 16 / 11 Aug 2025 / Optics Express 33715
Optics EXPRESS

Unidirectional Raman emission of Stokes photons from a circularly polarized transition of atoms in a chiral ring cavity

HAOLE JIAO,[1,2] MINJIE WANG,[1,2] MINGYUAN CHEN,[3] JIAJIN LU,[1,2] CAN SUN,[1,2] ZHIFANG YANG,[1,2] MENGQI XI,[1,2] SHUJING LI,[1,2] SHENGZHI WANG,[4] AND HAI WANG[1,2,*]

[1]State Key Laboratory of Quantum Optics Technologies and Devices, Shanxi University, Taiyuan 030006, China
[2]Collaborative Innovation Center of Extreme Optics, Shanxi University, Taiyuan 030006, China
[3]College of Engineering and Applied Sciences, Nanjing University, Nanjing 210023, China
[4]School of Physics and Information Engineering, Shanxi Normal University, Taiyuan 030031, China
[*]wanghai@sxu.edu.cn

Abstract: In this study, we demonstrated unidirectional Raman emission from cold ^{87}Rb atoms with a ring cavity. A bias magnetic field B_0 is applied along the z direction to define the quantization axis. By transversely applying pumping laser pulses on a π-transition of the atoms, we generate spontaneous Raman emissions of Stokes photons from an individual circularly polarized (σ^+) transition. The emissions are coupled into the running-wave cavity where two quarter-wave plates are inserted. We observed that the Stokes field is right-hand-circularly (left-hand-circularly) polarized when propagating along the z (–z) direction. The measured polarization extinction of the Stokes field escaped from the ring cavity is beyond 1400:1. A polarization interferometer is inserted in the cavity and the two orthogonal polarization modes are spatially split when propagating in the interferometer. By blocking one arm of the interferometer, we demonstrated a chiral cavity system with the atoms in the presence of the magnetic field. On this basis, we demonstrated unidirectional Raman emissions of Stokes photons in the ring cavity. The unidirectional factor reaches ~99.8%.

© 2025 Optica Publishing Group under the terms of the Optica Open Access Publishing Agreement

1. Introduction

A long-term task in optical quantum information science is to develop the techniques that can enable light–matter interactions in nonreciprocal ways [1,2]. Chiral quantum light–matter interfaces enable nonreciprocal coupling of quantum emitters (atoms) with photons, where the atoms emit (scatter, absorb) photons in forward and backward directions in an asymmetric way [1]. Based on the chiral quantum interfaces, schemes of [2–4] the chiral quantum networks or simulations of many body physics [5] have been proposed. Recently, unidirectional (forward- or backward-direction) light emissions from the circularly polarized transitions of a quantum emitter, which is set close to or embedded in nanophotonic waveguides, have been demonstrated [6–10]. Theoretical studies on the directionality of photon transport in waveguides have been reported [11,12]. A quantum optical circulator has been demonstrated with a system built with a single chiral atom coupled to a whispering-gallery-mode (WGM) microresonator [13]. These demonstrations are based on the locking between the spin and propagation directions of light fields that are transversely confined by nanophotonic devices [1,14]; this represents a quantum spin Hall effect of light [15]. Additionally, a nonreciprocal photon device was demonstrated in a WGM microresonator with Kerr nonlinearity [16]. However, in these schemes, the quantum emitters are set close to the dielectric surfaces, which perturb the strong atom–photon interaction [4]. In cavity optomechanical systems, chiral light–matter interactions have been

#567770 https://doi.org/10.1364/OE.567770
Journal © 2025 Received 2 Jun 2025; revised 5 Jul 2025; accepted 10 Jul 2025; published 31 Jul 2025

Optics EXPRESS

proposed for generating quantum nonreciprocal squeezing [17] and nonreciprocal entanglement [18], respectively. Recently, nonreciprocal quantum correlations have been experimentally demonstrated with light-atom system [19]. Additionally, cavity-enhanced chiral eigenmode spectroscopy has been demonstrated with a chiral material [20].

It has been known that the couplings (interactions) of cold and ultracold atomic ensembles with light fields can be effectively enhanced by optical cavities and may reach a strong-coupling level with a high-finesse cavity [21]. In the past two decades, atom-cavity systems have been used as important tools to investigate quantum information science [22–35], and single-photon-level isolators [36,37]. It has been well known that the circularly polarized transition of atoms is effectively coupled with circularly polarized light [38]. However, unidirectional (forward- or backward-direction) photon emissions from atoms have not been demonstrated via the chiral atom-photon coupling in a cavity.

In the present experiment, we demonstrated unidirectional emission of Stokes photons emitting from an individual circularly polarized transition of ^{87}Rb atoms coupled to a chiral ring cavity. This result relies on two key points. One is the handedness–momentum correlation of the Stokes emissions, which denotes that the Stokes field is right-hand-circularly (RHC) polarized when propagating along the z direction, and left-hand-circularly (LHC) when propagating in the –z direction. The other is the chiral cavity system integrated with two quarter-wave plates and a polarization interferometer with one arm being blocked.

2. Handedness–momentum correlation of the Stokes emissions

For understanding our scheme of the unidirectional Raman emission of Stokes photons, we firstly explain the handedness–momentum correlation of the Stokes emissions from a circularly polarized transition of cold ^{87}Rb atoms. Figure 1 shows the relative atomic levels. A bias magnetic field $B_0 \approx 4G$ is applied on the atoms along the z-axis to define the quantization axis of the atoms. The ^{87}Rb atoms are cooled and trapped by a Magneto-Optical Trap (MOT). After the atoms are released, they are initially prepared in the $|g\rangle = |5S_{1/2}, F = 2, m_g = 2\rangle$ state via optical pumping, where m_g denotes the magnetic quantum number. By applying pumping laser pulses that are tuned on the $|g\rangle \rightarrow |e\rangle$ transition along the x-axis (Fig. 1), spontaneous Raman emissions of Stokes photons are generated on the circularly polarized (σ^+) transition $|e\rangle \leftrightarrow |s\rangle$ with $\Delta m = m_e - m_s = 1$, where $|e\rangle = |5P_{1/2}, F' = 2, m_e = 2\rangle$ is the excited state, $|s\rangle = |5S_{1/2}, F = 1, m_s = 1\rangle$ is the ground state, and the pumping and Stokes transitions form a three-level Λ configuration. According to the selection rule [39], the σ^+ transition $\Delta m = 1$ effectively couples with the circularly polarized light field $\vec{E} = E_0 \frac{\vec{e}_x + i\vec{e}_y}{\sqrt{2}}$, where $\vec{e}_x$ ($\vec{e}_y$) denotes the unit vector along the x-axis (y-axis). The Stokes field emitting in the + z (-z)-direction is rewritten as $\vec{E}_k^{(R)} = E_0 \frac{\vec{e}_x + i\vec{e}_y}{\sqrt{2}} e^{-ikz}$ ($\vec{E}_{-k}^{(L)} = E_0 \frac{\vec{e}_x + i\vec{e}_y}{\sqrt{2}} e^{ikz}$), where k ($-k$) denotes the wave vector. The spins of the optical fields are related to their propagation directions. The forward-propagating field is RHC polarized [39] and then is written as $\vec{E}_k^{(R)} = E_0 \frac{\vec{e}_x + i\vec{e}_y}{\sqrt{2}} e^{-ikz}$, whereas the backward-propagating field is LHC polarized then is written as $\vec{E}_{-k}^{(L)} = E_0 \frac{\vec{e}_x + i\vec{e}_y}{\sqrt{2}} e^{ikz}$; these polarizations are intuitively shown in Fig. 1.

As discussed above, the two Stokes fields propagating along + z and –z directions have the inequality relation $\vec{E}_k \neq (\vec{E}_{-k})^*$, which violates the time-reversal symmetry. We explain this violation in the following.

For the light-matter interaction system with time-reversal symmetry, Maxwell's equations require that $E_k = E_{-k}^*$, where k and –k denotes the forward and backward propagating modes. Thus, the direction of spin is flipped and handedness is preserved [8,40]. In the atom–photon coupling with an external magnetic field B_0 being applied, the time-reversal symmetry will be broken [41]. Considering the case in which the external bias magnetic field B0 is not applied, the

Optics EXPRESS

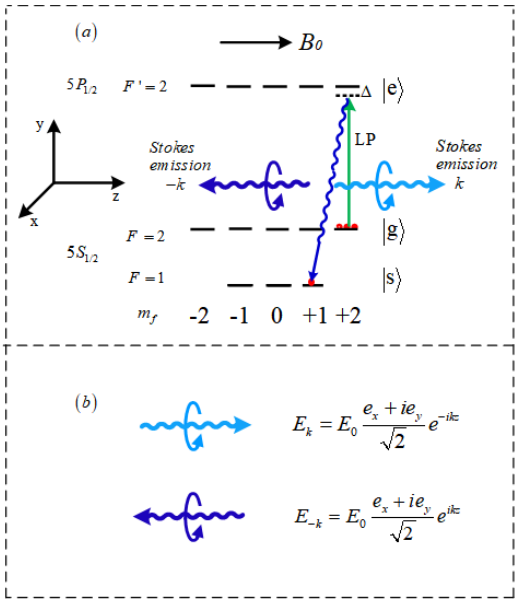

Fig. 1. (a) Relative atomic levels used for the Stokes emission, where, LP: laser pulses. (b) Relationship between the expression and chirality as well as the propagation directions of circularly polarized light.

Hamiltonian H_{a-p} of the coupling between the atoms and the Stokes emission field is written as:

$$H_{a-p} = \frac{1}{2m}\left(p - \frac{q}{c}A_p\right)^2 + V(r) \tag{1}$$

where p is the momentum operator of the electron in the individual atoms, q is the charge of an electron, c is the speed of light, m is the mass of the electron, $V(r)$ (r) is the Coulomb potential (position coordinate) of the electron in an individual atom, $A_p = A_{p0}e^{-i\omega_S t - ikz}$ is the vector potential of the Stokes field, and ω_S is the frequency of the Stokes field. The interaction Hamiltonian H_{a-p} for individual atoms and photons can be rewritten as follows:

$$H_{a-p} = H_0 - \frac{q}{mc}p \cdot A_p + \frac{q^2}{2mc^2}A_p^2 \tag{2}$$

where, $H_0 = \frac{p^2}{2m} + V(r)$ is the Hamiltonian of the individual atoms, and the term $\frac{q^2}{2mc^2}A_p^2$ is very small and negligible. Then, we have:

$$H_{a-p} \approx H_0 - \frac{q}{mc}p \cdot A_p \tag{3}$$

The time reverse operation of the Hamiltonian H_{a-p} is given by:

$$TH_{a-p}T^{-1} = TH_0T^{-1} - \frac{q}{mc}T(pA_p)T^{-1} = H_0 - \frac{q}{mc}(-p)(-A_p) = H_{a-p} \tag{4}$$

where $TA_pT^{-1} = -A_p$ [42]. Equation (4) shows that the atom–photon coupling in the absence of the bias magnetic field is time–reversal symmetry.

Optics EXPRESS

When the external bias magnetic field B0 is applied z-axis, the Hamiltonian for the individual atom–photon systems is rewritten as follows:

$$\begin{aligned} H'_{a-p} &= \frac{1}{2m}\left(p - \frac{q}{c}A_P - \frac{q}{c}A_0\right)^2 + V(r) \\ &\simeq H_0 - \frac{q}{mc}pA_P - \frac{q}{mc}pA_0 = H_{a-p} - \frac{q}{mc}pA_0 \end{aligned} \tag{5}$$

where $A_0 = \frac{1}{2}B_0 \times r$ is the vector potential of the bias magnetic field B_0. The time reverse operation of the Hamiltonian H'_{a-p} is given by:

$$TH'_{a-p}T^{-1} = TH_{a-p}T^{-1} - \frac{q}{mc}TpT^{-1}TA_0T^{-1} = H_{a-p} - \frac{q}{mc}(-p)A_0 = H_{a-p} + \frac{q}{mc}pA_0 \neq H'_{a-p} \tag{6}$$

In Eq. (6), B_0 (A_0) doesn't involve in the time inverse ($TA_0T^{-1} = A_0$) since it is to be as an external magnetic field.

3. Experimental results

Figure 2 shows a sketch of the experimental set up, which includes a cold atomic ensemble that is coupled to a ring cavity inserted with a polarization interferometer (PI). The ring cavity is formed by four flat mirrors M1, 2, 3 and the OCM, where the M1, 2, 3 mirrors have high reflections, and the mirror OCM is an output coupler that has a reflectance of 80%. The PI is formed by two beam displacers BD_1 and BD_2 [43]. The cold-atom (^{87}Rb) ensemble is inserted into an arm along the z-axis of the cavity. The quantization axis of the atoms is defined by the bias of the magnetic field $B_0 \approx 4G$ along the z-axis. Two quarter-wave plates $(\lambda/4)_1$ and $(\lambda/4)_2$ as well as two lenses (L1 and L2) are inserted at either end of the ensemble. The quarter-wave plates are used to change the Stokes field polarizations (see below for details), and the two lenses to focus the cavity modes into a small spot size of 1 mm at the center of the atoms. The cavity has a length of $\sim 5.5m$, a finesse of $F \approx 17$, a free spectral range FSR $\approx$ 55 MHz, and a line bandwidths of $\sim$3 MHz. In the present experiment, a locking laser beam with a large detuning ($\sim$600 MHz) from the atomic transition $|g\rangle = |5S_{1/2}, F = 2\rangle \leftrightarrow |e\rangle = |5P_{1/2}, F = 2\rangle$ is coupled into the ring cavity to stabilize the cavity length using Pound-Drever-Hall (PDH) method. The CW mode is made to resonate with the ring cavity by precisely adjusting the cavity length. We control the temperature of BD to let the CW and CCW modes resonate with the cavity at the same time.

We firstly experimentally observe the handedness–momentum correlation of the Stokes emissions. The experiment is carried out in a cyclic fashion. At the beginning of a trial, a 795-nm H-polarized pumping laser pulse with the red-detuned by $\Delta \approx 20$ MHz to the $|g, m_g = 2\rangle \rightarrow |e, m_e = 2\rangle$ transition is transversely applied to the atoms along y-axis (see Fig. 1). The pulse width is $\delta t \approx 250$ ns. This pumping pulse induces spontaneous emission of the Stokes photons on the circularly polarized transition $|e, m_e = 2\rangle \rightarrow |s, m_s = 1\rangle$ ($\Delta m = 1$), which corresponds to the DLCZ write process [44]. Emitting from the individual σ^+ transition, the Stokes field $\vec{E}_k^{(R)}$ propagating along the z direction and the Stokes field $\vec{E}_{-k}^{(L)}$ along the -z direction are coupled to the CW and CCW modes, respectively. Constrained to the handedness–momentum correlation, the Stokes emission from the circularly-polarized transition is RHC (LHC) polarized when it propagates along the z (–z) direction. They pass through the quarter-wave plates $[\lambda/4]_1$ and $[\lambda/4]_2$, respectively. The RHC polarized $\vec{E}_k^{(R)}$ field is changed into a H-polarized field labeled $\vec{E}_k^{(H)}$ after $[\lambda/4]_1$, and the LHC polarized $\vec{E}_{-k}^{(L)}$ field is changed into a V-polarized field $\vec{E}_{-k}^{(V)}$ after $[\lambda/4]_2$. The field $\vec{E}_{+k}^{H}$ ($\vec{E}_{-k}^{(V)}$) pass through the arm 1 (arm 2) of polarization interferometer (PI) along CW (CCW), (see Fig. 3). Subsequently, the polarization of $\vec{E}_{+k}^{H}$ ($\vec{E}_{-k}^{(V)}$) is changed back into RHC (LHC) -polarization after $[\lambda/4]_2$ ($[\lambda/4]_1$) . Both fields are coupled into the atoms again.

Optics EXPRESS

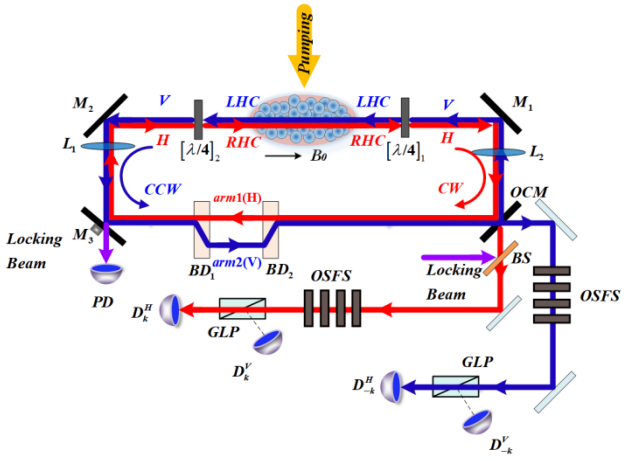

Fig. 2. Experimental set up. The forward (k) and backward (–k) emissions are coupled into the clockwise (CW, red line) and counterclockwise (CCW, blue line) modes of the cavity, respectively. A locking laser pulse is coupled to the cavity mode through the beam splitter (BS). Its leakage from the mirror M3 is used to stabilize the cavity length by using PDH method. GLP: Glan-Laser Prism; OSFS: Optical-Spectrum-Filter Set; BD1, BD2: Beam Displacers; OCM: Output coupler mirror; D_k^H, (D_{-k}^H) and D_k^V (D_{-k}^V): Single photon detectors for detecting H-polarization and V-polarization components propagating along k (-k).

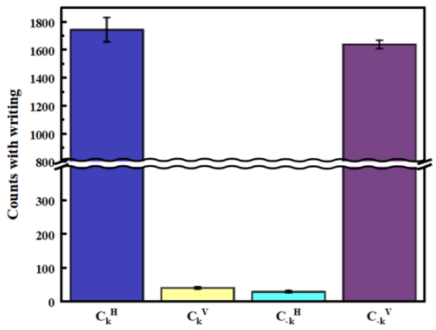

Fig. 3. Measured counts $C_k^{(H)}$, $C_{-k}^{(H)}$, $C_k^{(V)}$ $C_{-k}^{(V)}$ for 30 s at an excitation probability $\chi_k = \chi_{-k} \sim 1\%$. Error bars represent 1 standard deviation.

The couplings of the atoms to the Stokes fields in the cavity are enhanced by a factor of $2F/\pi$ via the Purcell effect.

To verify the handedness–momentum correlation, we measured the polarization extinction of the Stokes photons outputs at output coupler mirror (OCM) of the cavity. The Stokes field outputs propagating along the z- (–z-) direction are directed into polarization beam splitter—specifically Glan-Laser Prisms labeled GLP_{+k} (GLP_{-k}) —which transmits H-polarized light and reflects V-polarized light with >50 dB extinction ratio, directing to single-photon detectors of $D_k^{(H)}$ and $D_k^{(V)}$ ($D_{-k}^{(H)}$ and $D_{-k}^{(V)}$), respectively.

We use the ratio $\eta_k^{(R/L)} = \gamma_k^{(R)}/\gamma_k^{(L)}$ ($\eta_{-k}^{(R/L)} = \gamma_{-k}^{(R)}/\gamma_{-k}^{(L)}$) to characterize the polarization extinction of the Stokes fields along the z–direction (-z–direction), where $\gamma_k^{(R)}$ ($\gamma_k^{(L)}$) and $\gamma_{-k}^{(R)}$ ($\gamma_{-k}^{(L)}$) denote the spontaneous emission rates of the atoms emitting RHC (LHC)-polarization

Optics EXPRESS

photons into the CW and CCW modes. As mentioned above, the RHC-polarized (LHC-polarized) emission fields are transformed into H (V) polarization. The H (V)-polarization outputs from the cavity are directed to $D_k^{(H)}$ or $D_{-k}^{(H)}$, ($D_k^{(V)}$ or $D_{-k}^{(V)}$). Therefore, in our experiment, the emission rates can be measured as follows: $\gamma_k^{(R)} \propto C_k^{(H)} - N_k^{(H)}$, $\gamma_k^{(L)} \propto C_k^{(V)} - N_k^{(V)}$, $\gamma_{-k}^{(R)} \propto C_{-k}^{(H)} - N_{-k}^{(H)}$ and $\gamma_{-k}^{(L)} \propto C_{-k}^{(V)} - N_{-k}^{(V)}$, where $C_\alpha^{(X)}$ denotes the photon counts at the detector $D_\alpha^{(X)}$. $N_k^{(H)}$, $N_k^{(V)}$, $N_{-k}^{(H)}$, and $N_{-k}^{(V)}$ are the background noise at the detector $D_\alpha^{(X)}$ with $X = H, V$ and $\alpha = k, -k$, which are measured count values without the pumping laser pulse. For an excitation probability $\chi_k = \chi_{-k} \sim 1\%$ of generating a Stokes photon along the z or -z direction induced by a pumping pulse, we measured the cavity outputs using the detectors, and the measured $C_k^{(H)}$, $C_k^{(V)}$, $C_{-k}^{(H)}$ and $C_{-k}^{(V)}$ counts values during 30 s are plotted as histograms in Fig. 3, which are $C_k^{(H)} = 1746 \pm 87$, $C_k^{(V)} = 41 \pm 3$, $C_{-k}^{(H)} = 29 \pm 3$, $C_{-k}^{(V)} = 1641 \pm 30$. During the same time (30 s), the measured background-noise counts are $N_k^{(H)} \approx 85 \pm 8$, $N_k^{(V)} \approx 40 \pm 3$, $N_{-k}^{(H)} \approx 28 \pm 3$, and $N_{-k}^{(V)} \approx 12 \pm 2$, which correspond to background-noise probabilities per pulse to be $p_k^{(H)} \approx 4.25 \times 10^{-4}$, $p_k^{(V)} \approx 2 \times 10^{-4}$. $p_{-k}^{(H)} \approx 1.4 \times 10^{-4}$, and $p_{-k}^{(V)} \approx 6 \times 10^{-5}$, respectively.

From Fig. 3, we calculate the polarization extinction $\eta_k^{(R/L)} = \gamma_{+k}^{(R)}/\gamma_{+k}^{(L)} = \frac{C_k^{(H)} - N_k^{(H)}}{C_k^{(V)} - N_k^{(V)}} \approx 1480 : 1$ and $\eta_{-k}^{(R/L)} = \frac{(C_{-k}^{(H)} - N_{-k}^{H})}{(C_{-k}^{(V)} - N_{-k}^{V})} \approx 1 : 1440$. The measured results clearly show that the Stokes fields propagating along the z and –z directions are RHC and LHC polarizations, respectively. The forward and backward spontaneous emissions have the same spins and opposite handedness, which verify the time-reversal symmetry is broken [42,45]. As explained above, the handedness–momentum correlation describes the light emissions on a circularly polarized transition. This requires that time-reversal symmetry (Lorentz reciprocity) is broken by a bias magnetic field [41,46–48]. The magnetic field should be applied along a specific direction (z-axis in the present experiment) to define the quantization axis, whose value should be far beyond the residual magnetic field. In the ideal case, the bias magnetic field could be very weak. However, in practical experiments, there are residual (fluctuation) magnetic fields around atoms. So, one has to apply a stronger bias magnetic field to suppress the residual magnetic fields. In the present experiment, the measured residual magnetic field is ~20 mG and the bias magnetic field is $B_0 \approx 4G$, which is far beyond the measured residual magnetic field.

We subsequently demonstrated unidirectional Raman emission of Stokes photons in the ring cavity by dissipating the V- or H-polarization mode in the ring cavity. By setting an optical blocker in the arms 2 or 1 of the PI, respectively, we dissipate the V- or H- polarization modes and demonstrate forward- or backward-direction Stokes emission, respectively. When the V-polarized CCW mode (passing through the arm 2) is blocked, the counts of $C_k^{(H)}$, $C_k^{(V)}$, $C_{-k}^{(H)}$ and $C_{-k}^{(V)}$ measured by the detectors of $D_k^{(H)}$, $D_k^{(V)}$, $D_{-k}^{(H)}$ and $D_{-k}^{(V)}$ during 30 s are shown in the histogram in Fig. 4(a), which are $C_k^{(H)} = 1713 \pm 74$, $C_k^{(V)} = 41 \pm 3$, $C_{-k}^{(H)} = 29 \pm 3$, $C_{-k}^{(V)} = 13 \pm 2$. From these data, we obtain the ratio:$\gamma_k^{(R)} : \gamma_k^{(L)} : \gamma_{-k}^{(R)} : \gamma_{-k}^{(L)} \propto (C_k^{(H)} - N_k^{H}) : (C_k^{(V)} - N_k^{(V)}) : (C_{-k}^{(H)} - N_{-k}^{H}) : (C_{-k}^{(V)} - N_{-k}^{V}) \approx 1450 : 1 : 1 : 1$, which shows that the Stokes emission only propagates in the CW mode.

When the H-polarized CW mode (passing through the arm 1) is blocked, the measured $C_k^{(H)}$, $C_{-k}^{(H)}$, $C_k^{(V)}$, and $C_{-k}^{(V)}$ counts values during 30 s are plotted as histograms in Fig. 4(b), which are $C_k^{(H)} = 86 \pm 6$, $C_k^{(V)} = 41 \pm 3$, $C_{-k}^{(H)} = 29 \pm 3$, $C_{-k}^{(V)} = 1618 \pm 30$. From these data, we obtain the following ratio: $\gamma_k^{(R)} : \gamma_k^{(L)} : \gamma_{-k}^{(R)} : \gamma_{-k}^{(L)} \propto (C_k^{(H)} - N_k^{H}) : (C_k^{(V)} - N_k^{(V)}) : (C_{-k}^{(H)} - N_{-k}^{H}) : (C_{-k}^{(V)} - N_{-k}^{V}) \approx 1 : 1 : 1 : 1600$, which shows that the Stokes emission only propagates in the CCW mode.

Optics EXPRESS

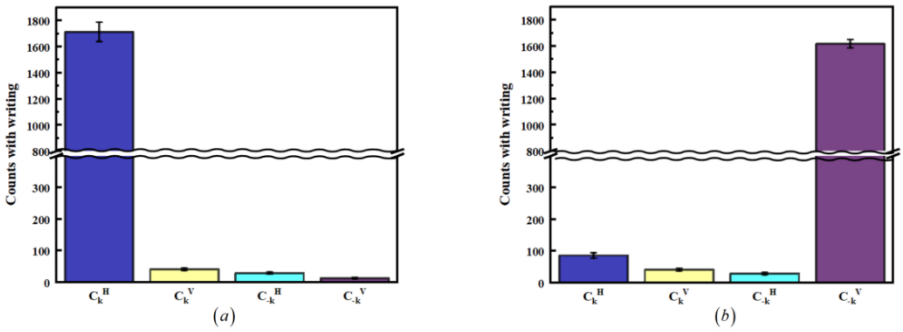

Fig. 4. Measured counts $C_k^{(H)}$, $C_{-k}^{(H)}$, $C_k^{(V)}$ $C_{-k}^{(V)}$ for a time of 30 seconds. (a) The arm2 of the polarization interferometer in the cavity is blocked, and the excitation probability of the CW mode is set $\chi_k \sim 1\%$. (b) The arm1 of the polarization interferometer in the cavity is blocked, and the excitation probability of the CCW mode is set $\chi_{-k} \sim 1\%$. Error bars represent 1 standard deviation.

The unidirectional emission in the cavity can be described by the directional β factor, which is defined as the ratio of the spontaneous emission rate into the ± k mode pair and the total emission rate [1]: $\beta_\pm = (\gamma_{\pm k}^{(R)} + \gamma_{\pm k}^{(L)})/(\gamma_{+k}^{(R)} + \gamma_{+k}^{(L)} + \gamma_{-k}^{(R)} + \gamma_{-k}^{(L)} + \Gamma)$, where Γ is the emission rate into all other modes. Since the cavity in the present experiment has a low finesse (~17), the emission rate Γ is far beyond that of the ± k modes ($\Gamma >> \gamma_{\pm k}$), and the directional β factor is close to zero. When a high-finesse cavity is used, strong atom–photon coupling causes the spontaneous emission rate Γ to approach zero. In this case, $\beta_+ \rightarrow 1$ and $\beta_- \rightarrow 0$ (or $\beta_- \rightarrow 1$ and $\beta_+ \rightarrow 0$); this represents ideal unidirectional emission. For our experiment, we define the unidirectional factor, which is written as $\beta_+' = (\gamma_+^{(R)} + \gamma_+^{(L)})/(\gamma_{+k}^{(R)} + \gamma_{+k}^{(L)} + \gamma_{-k}^{(R)} + \gamma_{-k}^{(L)})$ ($\beta_-' = (\gamma_-^{(R)} + \gamma_-^{(L)})/(\gamma_{+k}^{(R)} + \gamma_{+k}^{(L)} + \gamma_{-k}^{(R)} + \gamma_{-k}^{(L)})$), to describe the ratio of the escaped spontaneous emission from CW (CCW)-mode in the cavity to the total emission in both modes. Figure 4 shows that $\beta_+' \approx 99.86\%$ and $\beta_-' \approx 99.87\%$, which clearly show perfect unidirectional emission in the chiral atom-cavity system.

As discussed above, a key factor of achieving the unidirectional emissions of Stokes fields in the cavity is that the ring cavity system is set to be chiral. In the present experiment, we take the following steps for this. We insert two quarter-wave plates, which transform the circularly-polarized emissions from the atoms into linear-polarized ones. Additionally, we insert the PI in the cavity, which splits the two linear polarization modes into different spatial modes arm 1 and arm 2. Constrained to Lorentz time reversion, the light field with a specific circularly polarization at the atomic ensemble will be coupled into the same arm regardless of its propagating along z or –z –direction. For example, the RHC-polarized Stokes field propagating along z-direction at the ensemble will pass through the arm1, which has been described above. If the Stokes field is RHC-polarized but propagates along -z-direction, it will be changed into H-polarization after passing through the quarter-wave plates $[\lambda/4]_2$, and still propagate in the arm 1. In the present experiment, we block one of the spatial modes (the arm 1 or arm 2), only a specific circularly-polarized Stokes field is supported by the cavity, which demonstrates a chiral cavity system with the atoms in the prensence of magnetic field.

4. Conclusion

With ^{87}Rb cold atoms being coupled to a ring cavity, we observed high-precise handedness–momentum correlation of the Stokes emissions from an individual circularly polarized transition of atoms. Also, the application of the bias magnetic field along the z-axis clearly

Optics EXPRESS

defines the quantization axis, which makes the forward and backward Stokes emissions to be circularly-polarized light and promise us to demonstrate the chiral Raman emissions. The polarization excitations of the Stokes field in the CW or CCW mode is beyond 1400:1. We set the ring cavity to be chiral by inserting the PI and the quarter-wave plates in it. Recently, optical isolations have been demonstrated with atoms in a cavity [36,49], where, an input light beam propagating in forward direction can pass through the isolator and the beam propagating in backward direction will be blocked. In contrast to these works, we demonstrated the unidirectional Raman emissions of Stokes photons from atoms in the chiral cavity system with the atoms in the prensence of magnetic field. The unidirectional factor is measured, which reaches ~99.8%. The demonstrated unidirectional Raman emissions of Stokes photons in the ring cavity can be found in applications in chiral quantum networks [2], in directional phase-sensitive amplifiers [50], and in the suppression of backward spontaneous Raman scattering of Stokes photons in a standing-wave cavity [51].

Funding. Fund for Shanxi Key Subjects Construction (1331); National Natural Science Foundation of China (12174235).

Disclosures. The authors declare that they have no conflicts of interest.

Data availability. The data underlying the results presented in this paper are not publicly available at this time but may be obtained from the authors upon reasonable request.

References

1. P. Lodahl, S. Mahmoodian, S. Stobbe, *et al.*, "Chiral quantum optics," Nature **541**(7638), 473–480 (2017).
2. H. Pichler, T. Ramos, A. J. Daley, *et al.*, "Quantum optics of chiral spin networks," Phys. Rev. A **91**(4), 042116 (2015).
3. T. Ramos, B. Vermersch, P. Hauke, *et al.*, "Non-Markovian dynamics in chiral quantum networks with spins and photons," Phys. Rev. A **93**(6), 062104 (2016).
4. A. Grankin, P. O. Guimond, D. V. Vasilyev, *et al.*, "Free-space photonic quantum link and chiral quantum optics," Phys. Rev. A **98**(4), 043825 (2018).
5. T. Ramos, H. Pichler, A. J. Daley, *et al.*, "Quantum Spin Dimers from Chiral Dissipation in Cold-Atom Chains," Phys. Rev. Lett. **113**(23), 237203 (2014).
6. J. Petersen, J. Volz, and A. Rauschenbeutel, "Chiral nanophotonic waveguide interface based on spin-orbit interaction of light," Science **346**(6205), 67–71 (2014).
7. R. Mitsch, C. Sayrin, B. Albrecht, *et al.*, "Quantum state-controlled directional spontaneous emission of photons into a nanophotonic waveguide," Nat. Commun. **5**(1), 5713 (2014).
8. I. Söllner, S. Mahmoodian, S. L. Hansen, *et al.*, "Deterministic photon–emitter coupling in chiral photonic circuits," Nat. Nanotechnol. **10**(9), 775–778 (2015).
9. R. J. Coles, D. M. Price, J. E. Dixon, *et al.*, "Chirality of nanophotonic waveguide with embedded quantum emitter for unidirectional spin transfer," Nat. Commun. **7**(1), 11183 (2016).
10. K. Xia, G. Lu, G. Lin, *et al.*, "Reversible nonmagnetic single-photon isolation using unbalanced quantum coupling," Phys. Rev. A **90**(4), 043802 (2014).
11. I. M. Mirza, J. G. Hoskins, and J. C. Schotland, "Chirality, band structure, and localization in waveguide quantum electrodynamics," Phys. Rev. A **96**(5), 053804 (2017).
12. C.-H. Yan, M. Li, X.-B. Xu, *et al.*, "Unidirectional transmission of single photons under nonideal chiral photon-atom interactions," Phys. Rev. A **102**(5), 053719 (2020).
13. M. Scheucher, A. Hilico, E. Will, *et al.*, "Quantum optical circulator controlled by a single chirally coupled atom," Science **354**(6319), 1577–1580 (2016).
14. T. Van Mechelen and Z. Jacob, "Universal spin-momentum locking of evanescent waves," Optica **3**(2), 118–126 (2016).
15. K. Y. Bliokh, D. Smirnova, and F. Nori, "Quantum spin Hall effect of light," Science **348**(6242), 1448–1451 (2015).
16. R. Huang, A. Miranowicz, J.-Q. Liao, *et al.*, "Nonreciprocal Photon Blockade," Phys. Rev. Lett. **121**(15), 153601 (2018).
17. J. Wang, Q. Zhang, Y.-F. Jiao, *et al.*, "Quantum advantage of one-way squeezing in weak-force sensing," Appl. Phys. Rev. **11**(3), 031409 (2024).
18. Y.-F. Jiao, S.-D. Zhang, Y.-L. Zhang, *et al.*, "Nonreciprocal Optomechanical Entanglement against Backscattering Losses," Phys. Rev. Lett. **125**(14), 143605 (2020).
19. Z. Zhang, Z. Xu, R. Huang, *et al.*, "Chirality-induced quantum non-reciprocity," Nat. Photonics (2025).
20. W. Zhou, Y.-P. Ruan, H. Wu, *et al.*, "Magnetic-free chiral eigenmode spectroscopy for simultaneous sensitive measurement of optical rotary dispersion and circular dichroism," eLight **4**(1), 12 (2024).
21. A. Reiserer and G. Rempe, "Cavity-based quantum networks with single atoms and optical photons," Rev. Mod. Phys. **87**(4), 1379–1418 (2015).

Optics EXPRESS

22. Q. A. Turchette, C. J. Hood, W. Lange, *et al.*, "Measurement of Conditional Phase Shifts for Quantum Logic," Phys. Rev. Lett. **75**(25), 4710–4713 (1995).
23. J. I. Cirac, P. Zoller, H. J. Kimble, *et al.*, "Quantum State Transfer and Entanglement Distribution among Distant Nodes in a Quantum Network," Phys. Rev. Lett. **78**(16), 3221–3224 (1997).
24. A. Reiserer, N. Kalb, G. Rempe, *et al.*, "A quantum gate between a flying optical photon and a single trapped atom," Nature **508**(7495), 237–240 (2014).
25. M. Brekenfeld, D. Niemietz, J. D. Christesen, *et al.*, "A quantum network node with crossed optical fibre cavities," Nat. Phys. **16**(6), 647–651 (2020).
26. X.-H. Bao, A. Reingruber, P. Dietrich, *et al.*, "Efficient and long-lived quantum memory with cold atoms inside a ring cavity," Nat. Phys. **8**(7), 517–521 (2012).
27. J. Vaneecloo, S. Garcia, and A. Ourjoumtsev, "Intracavity Rydberg Superatom for Optical Quantum Engineering: Coherent Control, Single-Shot Detection, and Optical π Phase Shift," Phys. Rev. X **12**(2), 021034 (2022).
28. T. Stolz, H. Hegels, M. Winter, *et al.*, "Quantum-Logic Gate between Two Optical Photons with an Average Efficiency above 40%," Phys. Rev. X **12**(2), 021035 (2022).
29. N. Jia, N. Schine, A. Georgakopoulos, *et al.*, "A strongly interacting polaritonic quantum dot," Nat. Phys. **14**(6), 550–554 (2018).
30. N. Jia, A. Georgakopoulos, A. Ryou, *et al.*, "Observation and characterization of cavity Rydberg polaritons," Phys. Rev. A **93**(4), 041802 (2016).
31. S.-J. Yang, X.-J. Wang, J. Li, *et al.*, "Highly Retrievable Spin-Wave–Photon Entanglement Source," Phys. Rev. Lett. **114**(21), 210501 (2015).
32. C.-W. Yang, J. Li, M.-T. Zhou, *et al.*, "Deterministic measurement of a Rydberg superatom qubit via cavity-enhanced single-photon emission," Optica **9**(8), 853–858 (2022).
33. D. J. Saunders, J. H. D. Munns, T. F. M. Champion, *et al.*, "Cavity-Enhanced Room-Temperature Broadband Raman Memory," Phys. Rev. Lett. **116**(9), 090501 (2016).
34. L. Heller, P. Farrera, G. Heinze, *et al.*, "Cold-Atom Temporally Multiplexed Quantum Memory with Cavity-Enhanced Noise Suppression," Phys. Rev. Lett. **124**(21), 210504 (2020).
35. J. Simon, H. Tanji, J. K. Thompson, *et al.*, "Interfacing Collective Atomic Excitations and Single Photons," Phys. Rev. Lett. **98**(18), 183601 (2007).
36. P. Yang, M. Li, X. Han, *et al.*, "Non-Reciprocal Cavity Polariton with Atoms Strongly Coupled to Optical Cavity," Laser Photonics Rev. **17**(7), 2200574 (2023).
37. P. Yang, X. Xia, H. He, *et al.*, "Realization of Nonlinear Optical Nonreciprocity on a Few-Photon Level Based on Atoms Strongly Coupled to an Asymmetric Cavity," Phys. Rev. Lett. **123**(23), 233604 (2019).
38. C. J. Foot, *Atomic Physics* (Oxford University Press, 2005), Vol. 7, Chap. 1.
39. E. Hecht, A. Zajac, and M. E. Cox, "Optics," Am. J. Phys. **42**(10), 921–922 (1974).
40. R. Potton, "Reciprocity in optics," Rep. Prog. Phys. **67**(5), 717–754 (2004).
41. Y. Hadad, J. C. Soric, and A. Alu, "Breaking temporal symmetries for emission and absorption," Proc. Natl. Acad. Sci. **113**(13), 3471–3475 (2016).
42. C. Caloz, A. Alù, S. Tretyakov, *et al.*, "Electromagnetic Nonreciprocity," Phys. Rev. Appl. **10**(4), 047001 (2018).
43. M. Wang, S. Wang, T. Ma, *et al.*, "Generation of highly retrievable atom photon entanglement with a millisecond lifetime via a spatially multiplexed cavity," Quantum **7**, 903 (2023).
44. J. Laurat, K. S. Choi, H. Deng, *et al.*, "Heralded Entanglement between Atomic Ensembles: Preparation, Decoherence, and Scaling," Phys. Rev. Lett. **99**(18), 180504 (2007).
45. J. Koch, A. A. Houck, K. L. Hur, *et al.*, "Time-reversal-symmetry breaking in circuit-QED-based photon lattices," Phys. Rev. A **82**(4), 043811 (2010).
46. S. Yang, M. Liu, C. Zhao, *et al.*, "Nonreciprocal thermal photonics," Nat. Photonics **18**(5), 412–424 (2024).
47. Z. Zhang and L. Zhu, "Broadband Nonreciprocal Thermal Emission," Phys. Rev. Appl. **19**(1), 014013 (2023).
48. K. J. Shayegan, J. S. Hwang, B. Zhao, *et al.*, "Broadband nonreciprocal thermal emissivity and absorptivity," Light: Sci. Appl. **13**(1), 176 (2024).
49. N. Jia, N. Schine, A. Georgakopoulos, *et al.*, "Photons and polaritons in a broken-time-reversal nonplanar resonator," Phys. Rev. A **97**(1), 013802 (2018).
50. A. Metelmann and A. A. Clerk, "Nonreciprocal Photon Transmission and Amplification via Reservoir Engineering," Phys. Rev. X **5**(2), 021025 (2015).
51. Unpublished work.

318.26.34.85 2025-07-31 22:44:24